Communications

A Printed Dipole Antenna With Tapered Slot Feed for Ultrawide-Band Applications

Tzyh-Ghuang Ma and Shyh-Kang Jeng

***Abstract*—In this paper a planar antenna is studied for ultrawide-band (UWB) applications. This antenna consists of a wide-band tapered-slot feeding structure, curved radiators and a parasitic element. It is a modification of the conventional dual exponential tapered slot antenna and can be viewed as a printed dipole antenna with tapered slot feed. The design guideline is introduced, and the antenna parameters including return loss, radiation patterns and gain are investigated. To demonstrate the applicability of the proposed antenna to UWB applications, the transfer functions of a transmitting-receiving system with a pair of identical antennas are measured. Transient waveforms as the transmitting-receiving system being excited by a simulated pulse are discussed at the end of this paper.**

***Index Terms*—Dipole antennas, slot fed antennas, ultrawide-band antennas.**

I. Introduction

Ultrawide-band (UWB) technology has experienced a blooming growth in the past few years. The basic idea of this promising technology is to directly transmit and receive trains of extremely short pulses that spread over bandwidth of several GHz. In 2002, the Federal Communication Commission (FCC) in United States allocated the spectrum from 3.1 to 10.6 GHz with EIRP less than -41.3 dBm/MHz for unlicensed UWB applications. The antenna implemented in an UWB system is very distinct from those applied to the traditional narrowband systems [1]. In such a system, the antenna behaves like a bandpass filter and tends to reshape the spectrum of the baseband signals. Generally speaking, it is quite challenging to design an antenna to simultaneously fulfill all the requirements in an UWB system, which include ultrawide bandwidth, omnidirectional patterns, constant gain and group delay, high radiation efficiency, and low profile. Various literatures have been devoted to discussing the antennas for UWB systems [2]–[5], which include magnetic slot antennas, disc monopole antennas and tapered slot antennas.

The tapered slot antennas, belonging to traveling wave antennas with planar structures, exhibit wide-band characteristics [6], and are capable of transmitting baseband pulses with low distortions [5]. These antennas, however, may become unsatisfactory in UWB systems due to their inherently directional patterns. Recently, we reported an antenna that is a modification of the conventional dual exponentially tapered slot antennas [7], and can be viewed as a printed dipole antenna with tapered slot feed [8]. This antenna consists of a wide-band tapered-slot feeding structure and a pair of curved strips that can radiate energy more uniformly over the space. To improve the antenna in-band impedance matching, an additional parasitic element is added in front of the feeding aperture [9]. In this paper, a detailed study of this antenna is given, which includes the design guideline as well as the antenna performance. In Section II, the antenna geometry, design guideline, and parameters including return loss, radiation patterns and gain are introduced. The transfer functions of a transmitting-receiving system with a pair of identical antennas are discussed in Section III. As indicated in [1], this system transfer function is very useful in UWB antenna designs. To unveil how the pulses are distorted by such a system, the simulated transient waveforms are evaluated at the end of this paper.

Manuscript received August 19, 2003; revised March 2, 2005.

T.-G. Ma is with the Department of Electrical Engineering, National Taiwan University of Science and Technology, Taipei, Taiwan, R.O.C. (e-mail: tgma@ee.ntust.edu.tw).

S.-K. Jeng is with the Graduate Institute of Communication Engineering and Department of Electrical Engineering, National Taiwan University, Taipei, Taiwan, R.O.C. (e-mail: skjeng@ew.ee.ntu.edu.tw).

Digital Object Identifier 10.1109/TAP.2005.858819

II. Antenna Design and Performance

Fig. 1 illustrates the geometry of the proposed antenna with the associated parameters. The antenna lies in the xz-plane with its normal direction being parallel to the y-axis. The feeding slotline and the radiators are on the top layer of the substrate whereas the microstrip line and its open stub are printed on the bottom layer of it. The substrate is with height h and dielectric constant ε_r. The energy is first transferred from the microstrip line to the slotline by a wide-band transition [10]. A pair of curved strips is then attached to the slotline and forms a tapered-slot feeding structure. This feeding structure acts as a wide-band impedance transformer and guides the wave propagating from the slotline to the space without causing pernicious reflection. Unlike the conventional dual exponentially tapered slot antenna, in this design the outer part of the strips is curved backward to deliver part of the energy to the opposite side of the feeding aperture. The inner and outer boundaries of the strips are described by two ellipses, whose semi-major axes are equal to L_b and $L_b + W_s$, and semi-minor axes are equal to W_b and $W_b + W_s$, respectively. An additional parasitic element is added in front of the feeding aperture. This parasitic element alters the current distribution of the radiators and therefore has influence on the antenna input impedance. By suitably adjusting the location of this parasitic element, the antenna in-band impedance matching can be effectively improved [8].

In designing the antenna, the lowest operating frequency f_l is first estimated by

$$f_l = \frac{c}{\sqrt{\varepsilon_{\rm eff}} \cdot \lambda_l} \approx \frac{c}{\sqrt{\varepsilon_{\rm eff}} \cdot L_l} \tag{1}$$

where $L_l = \pi(\sqrt{((L_b + W_s)^2 + (W_b + W_s)^2)/2})$ is the approximated longest current path along the outer boundary of the curved strips, c is the speed of light and $\varepsilon_{\rm eff} = (\varepsilon_r + 1)/2)$ is the effective dielectric constant. After determining the lowest operating frequency, the dimension of the wide-band microstrip line-to-slotline transition is designed to maximize the antenna impedance bandwidth. The highest operating frequency f_u of the antenna is related to that of the wide-band transition. Finally, the distance from the parasitic element to the feeding aperture L_r is adjusted to improve the antenna in-band impedance matching. The length of the parasitic element, which only has minor effects on the antenna performance [8], is equal to $L_l/2$.

Following the design guideline, the proposed antenna was designed on a Rogers RT/Duroid 5880 substrate with $h = 1.57$ mm and $\varepsilon_r = 2.2$. The design parameters are summarized in the caption of Fig. 1. The dimension of this antenna is 71 by 86 mm^2. Fig. 2 illustrates the measured return loss of the antenna. Referring to the figure, the operating bandwidth with $|S_{11}| < -9.5$ dB (or VSWR < 2) covers almost the whole UWB spectrum from 3.1 to 10.6 GHz. The radiation

0018-926X/$20.00 © 2005 IEEE

Authorized licensed use limited to: National Taiwan University. Downloaded on January 19, 2009 at 22:41 from IEEE Xplore. Restrictions apply.

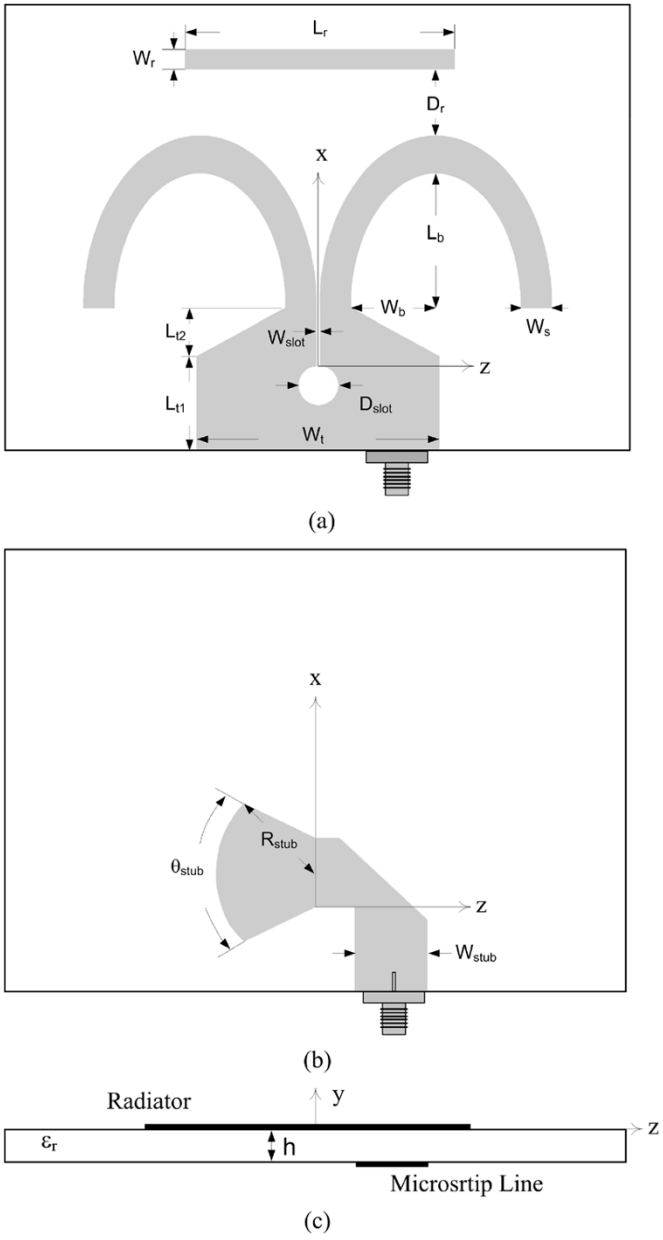

Fig. 1. Geometry of the antenna. (a) Top layer, (b) bottom layer, and (c) cross-sectional view. The design parameters are $L_b = 25$ mm, $W_b = 15$ mm, $W_s = W_r = 4$ mm, $L_r = 38.5$ mm, $D_r = 12$ mm, $W_{\rm slot} = 0.3$ mm, $D_{\rm slot} = 4$ mm, $W_{\rm stub} = 4.95$ mm, $r_{\rm stub} = 8$ mm, $\theta_{\rm stub} = 100°$, $W_t = 22$ mm, $L_{t1} = 12$ mm, and $L_{t2} = 7$ mm.

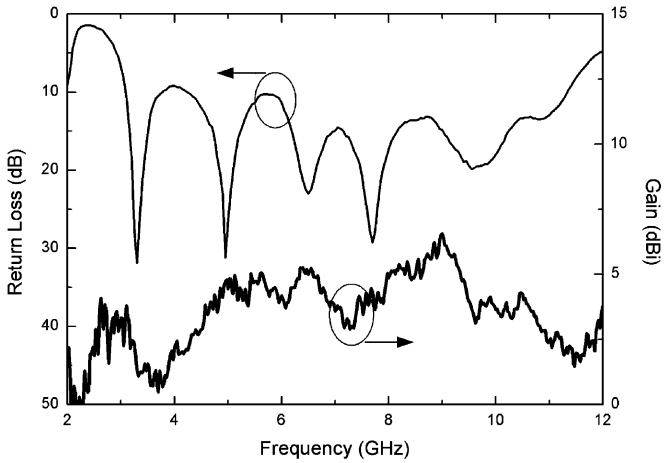

Fig. 2. Measured return loss and gain of the proposed antenna.

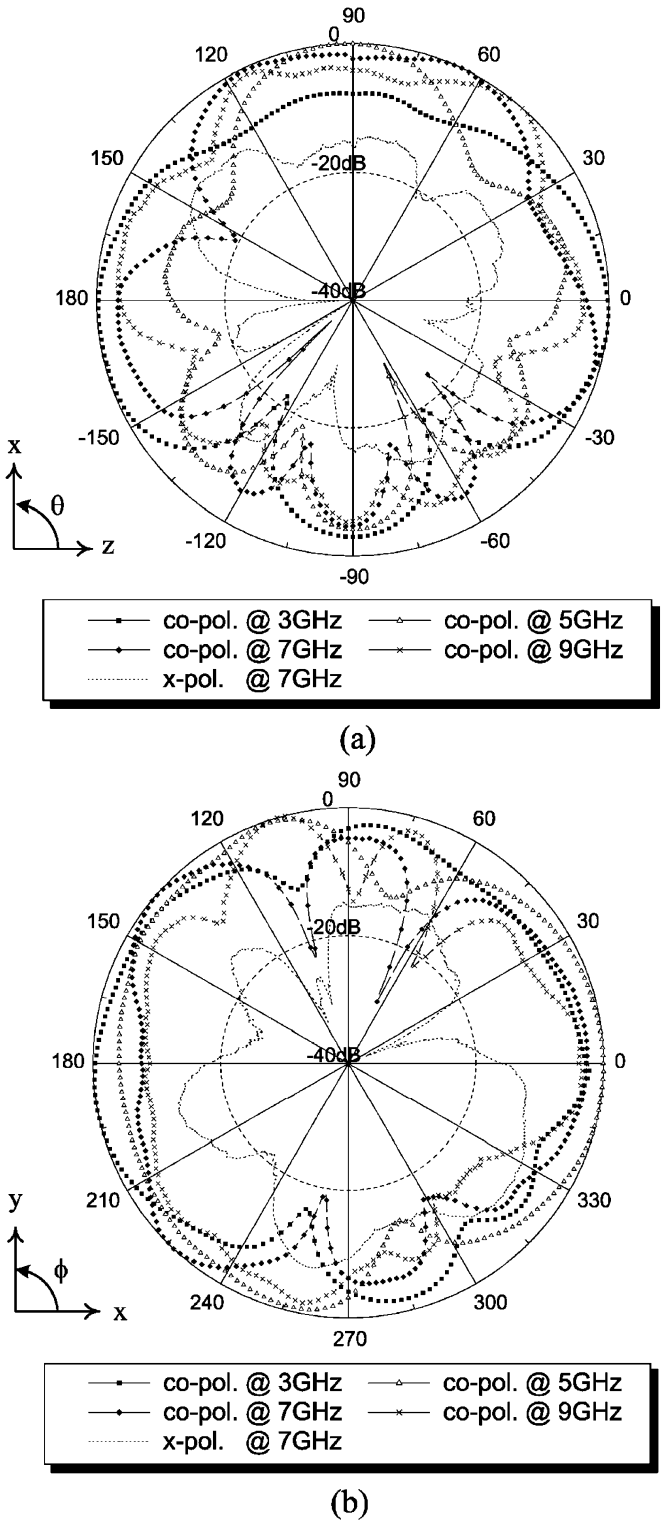

Fig. 3. Measured radiation patterns of the proposed antenna at 3, 5, 7, and 9 GHz. (a) E-plane and (b) H-plane.

patterns were measured in an anechoic chamber and calibrated with the standard two-antenna gain measurement method. The measured radiation patterns at 3, 5, 7, and 9 GHz in both E- (xz-) and H- (xy-) planes are illustrated in Fig. 3(a) and (b), respectively. Comparing to those of a conventional dual exponential tapered slot antenna, the radiation patterns of the proposed antenna are less directive as expected. Nevertheless, it is observed that the radiation patterns are not stable as the

Authorized licensed use limited to: National Taiwan University. Downloaded on January 19, 2009 at 22:41 from IEEE Xplore. Restrictions apply.

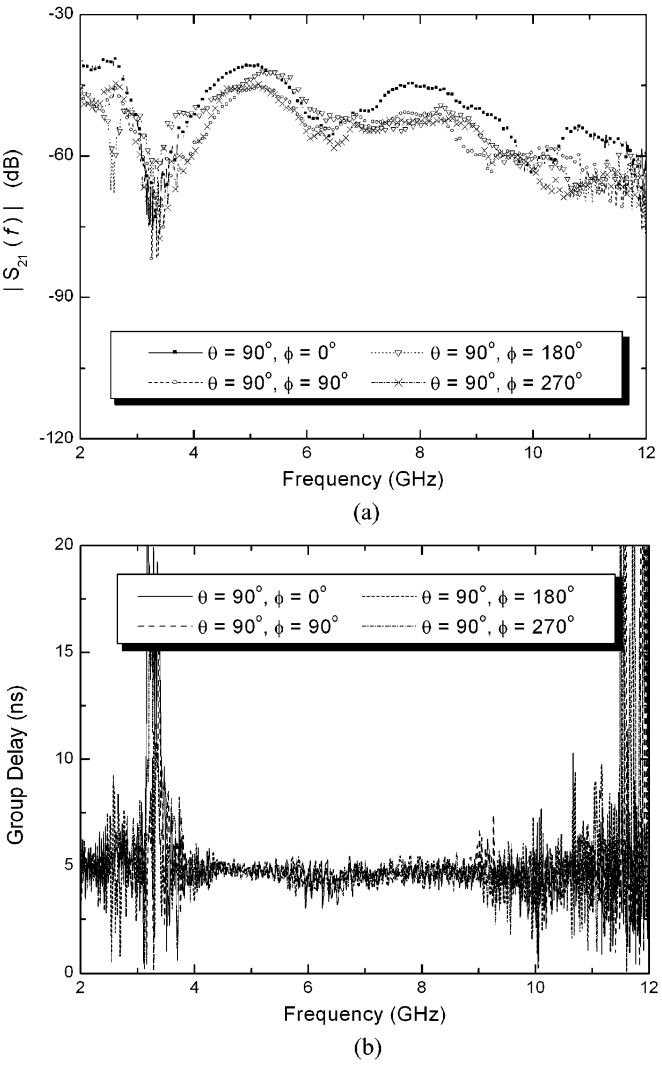

Fig. 4. (a) Magnitudes and (b) group delays of the measured system transfer functions at $\phi = 0°, 90°, 180°, 270°$, and $\theta = 90°$.

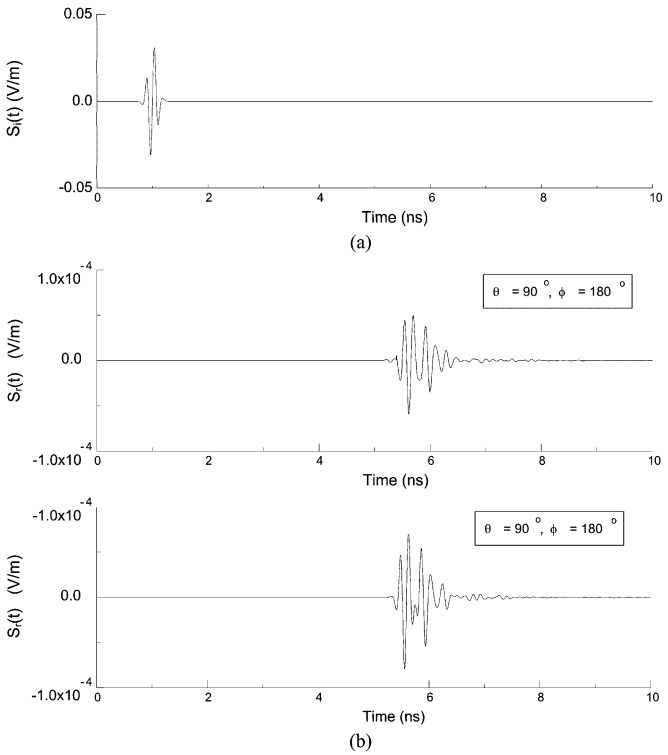

Fig. 5. (a) Simulated input pulse at the transmitting antenna terminal. (b) Evaluated transient waveforms at the receiving antenna terminal at $\phi = 0°$ and $180°$

frequency varies. This can be principally attributed to the variations of the current distributions on the radiating strips that may cause destructive interferences at certain frequencies. The reflections from the SMA connector may also have some influence. The antenna gain, which is depicted in Fig. 2, reveals a similar trend as well.

III. System Transfer Functions

In designing UWB antennas, it is insufficient to evaluate the antenna performance solely in traditional well-defined parameters like return loss, radiation patterns and gain, etc. Instead, as indicated in [1], it is crucial to evaluate the system transfer functions as the transmitting and receiving antennas are viewed as a whole system. For UWB applications, the magnitude of this transfer function should be as flat as possible in the operating band. The group delay is required to be constant over the entire band as well. A transmitting-receiving antenna system whose transfer functions satisfy these requirements will introduce limited distortions to baseband signals. In this paper, the system transfer function, which is in essence the transmission scattering parameter $S_{21}(f)$ of a two-port network, was measured in an anechoic chamber with a pair of proposed antennas serving as the transmitting and receiving antennas. The separation between the antenna apertures was 1.2 m. To eliminate the responses of the instruments the reference planes were calibrated to the antenna terminals in advance. Fig. 4(a) illustrates the magnitudes of the measured system transfer functions at $\phi = 0°, 90°, 180°, 270°$, and $\theta = 90°$. As shown in the figure, the variations of the system transfer functions are within 15 dB in most part of the operating band, but can be as high as 40 dB at the band edges. These nonflat responses inevitably introduce undesired distortions to baseband pulses. The measured group delays are shown in Fig. 4(b). Referring to the figure, the group delays are rather stable over the frequency band of interest.

To illustrate how the pulses are distorted by such a transmitting-receiving antenna system, in this paper the fifth derivative of a Gaussian pulse is chosen as the simulated input pulse at the transmitting antenna terminal, as shown in Fig. 5(a). The corresponding pulse spectrum completely complies with the FCC indoor emission mask. The transient waveform at the receiving antenna terminal can be achieved by performing an inverse Fourier transform on the product of this pulse spectrum and the measured system transfer function. Fig. 5(b) illustrates the received waveforms evaluated at $\phi = 0°$ and $180°$. Referring to the figure, the received pulses are distorted and broadened to more than 1ns. This also concludes that the nonflat system transfer functions dramatically affect the baseband signals.

IV. Conclusion

In this paper, an ultrawide-band printed dipole antenna with tapered slot feed has been proposed and demonstrated. The performance of this antenna has been experimentally investigated with the help of the well-defined antenna parameters as well as the transfer functions of a transmitting-receiving antenna system. The simulated transient waveforms are discussed as well. The future works will be in improving the unstable antenna radiation patterns as well as in further reducing the antenna dimension to give additional flexibility in circuit integrations.

Authorized licensed use limited to: National Taiwan University. Downloaded on January 19, 2009 at 22:41 from IEEE Xplore. Restrictions apply.

REFERENCES

[1] Z. N. Chen, X. H. Wu, N. Yang, and M. Y. W. Chia, "Considerations for source pulses and antennas in UWB radio systems," *IEEE Trans. Antennas Propag.*, vol. 52, no. 7, pp. 1739–1748, Jul. 2004.

[2] H. G. Schantz, "UWB magnetic antennas," in *IEEE AP-S Int. Symp. Dig.*, vol. 3, Columbus, OH, Jun. 2003, pp. 604–607.

[3] X. Qing, M. Y. W. Chia, and X. Wu, "Wide-slot antenna for UWB applications," in *IEEE AP-S Int. Symp. Dig.*, vol. 3, Columbus, OH, Jun. 2003, pp. 834–837.

[4] M. J. Ammann, "Improved pattern stability for monopole antennas with ultrawideband impedance characteristics," in *IEEE AP-S Int. Symp. Dig.*, vol. 1, Columbus, OH, Jun. 2003, pp. 818–821.

[5] W. Sorgel, C. Waldschmidt, and W. Wiesbeck, "Transient responses of a Vivaldi antenna and a logarithmic periodic dipole array for ultra wideband communication," in *IEEE AP-S Int. Symp. Dig.*, vol. 3, Columbus, OH, Jun. 2003, pp. 592–595.

[6] J. Shin and D. H. Schaubert, "A parameter study of stripline-fed Vivaldi notch-antenna arrays," *IEEE Trans. Antennas Propag.*, vol. 47, no. 5, pp. 879–886, May 1999.

[7] M. C. Greenberg, K. L. Virga, and C. L. Hammond, "Performance characteristics of dual exponentially tapered slot antenna (DETSA) for wireless communications applications," *IEEE Trans. Veh. Technol.*, vol. 52, no. 3, pp. 305–312, Mar. 2003.

[8] T. G. Ma and S. K. Jeng, "A parameter study of a novel ultra-wideband printed dipole antenna with tapered slot feed," in *Proc. Asia-Pacific Microwave Conf.*, vol. 3, Seoul, Korea, Nov. 2003, pp. 1981–1984.

[9] W. R. Deal, N. Kaneda, J. Sor, Y. Qian, and T. Itoh, "A new quasi-Yagi antenna for planar active antenna arrays," *IEEE Trans. Microw. Theory Tech.*, vol. 48, no. 6, pp. 910–918, Jun. 2000.

[10] B. Schuppert, "Microstrip/slotline transitions: Modeling and experimental investigation," *IEEE Trans. Microw. Theory Tech.*, vol. 36, no. 8, pp. 1272–1282, Aug. 1988.

EMC Internal Patch Antenna for UMTS Operation in a Mobile Device

Chih-Ming Su, Kin-Lu Wong, Chia-Lun Tang, and Shih-Huang Yeh

***Abstract*—A novel patch antenna suitable to be applied in a mobile device as an internal antenna having an electromagnetic compatibility (EMC) property with nearby conducting elements is presented. The antenna is easily fabricated from a single metal plate and mainly comprises a top patch and an inverted-L vertical ground wall. Due to the presence of the inverted-L ground wall, which is perpendicular to the system ground plane of the mobile device, the possible fringing EM fields in the surrounding region of the antenna are suppressed. In this case possible coupling between the antenna and the nearby conducting elements is expected to be small, and thus degrading effects on the performance of the antenna are eliminated. A design example of the proposed antenna for Universal Mobile Telecommunication System (UMTS) 1920–2170 MHz operation in a mobile device is demonstrated and discussed.**

***Index Terms*—Antennas, electromagnetic compatibility (EMC) antennas, internal mobile phone antennas, mobile antennas, Universal Mobile Telecommunication System (UMTS) antennas.**

I. INTRODUCTION

Conventional patch planar inverted-F antennas (PIFAs) mainly comprise a top radiating patch, a bottom ground plane, and a vertical feeding pin and a vertical shorting pin placed in between the top patch and the bottom ground [1]. This kind of patch PIFAs has been successfully applied as internal antennas in mobile devices, such as the mobile phone or Personal Digital Assistant (PDA) phone, for cellular communications [1]. However, with the configuration of the conventional patch PIFA, the side surfaces between the top patch and the bottom ground plane are open to exterior, thus allowing the fringing electromagnetic (EM) fields easily penetrated into the surrounding region of the antenna. In this case, strong coupling between the antenna and the nearby associated elements inside a mobile device will occur. This possible coupling will then cause degrading effects on the performance of the internal antenna. Thus, for practical applications, an isolation distance (usually at least 5 mm or even larger than 7 mm) is required such that the antenna performance will not be degraded due to the possible coupling effects.

To overcome the problem, we propose a new internal patch antenna EM compatible with the nearby associated conducting elements in a mobile device. The proposed antenna is designed to have an inverted-L vertical ground wall at the antenna's side surfaces, which can be expected to effectively suppress or eliminate the fringing EM fields in the surrounding region of the antenna. Thus, for applying the proposed internal antenna in a mobile device, the required isolation distance between the antenna and the nearby conducting elements will be no longer required. A design example of the proposed antenna for Universal Mobile Telecommunication System (UMTS) 1920–2170 MHz operation in a mobile device is demonstrated in the study. Details of the design considerations of the proposed antenna are described. Effects of the possible nearby conducting elements such as the RF/battery shielding metal case and the shielding metal

Manuscript received March 30, 2005.

C.-M. Su and K.-L. Wong are with the Department of Electrical Engineering, National Sun Yat-Sen University, Kaohsiung 80424, Taiwan, R.O.C.

C.-L. Tang and S.-H. Yeh are with the Computer and Communications Research Laboratories, Industrial Technology Research Institute, Hsinchu 310, Taiwan, R.O.C.

Digital Object Identifier 10.1109/TAP.2005.858827

0018-926X/$20.00 © 2005 IEEE

Authorized licensed use limited to: National Taiwan University. Downloaded on January 19, 2009 at 22:41 from IEEE Xplore. Restrictions apply.